Hindawi Publishing Corporation
International Journal of Antennas and Propagation
Volume 2015, Article ID 292905, 7 pages
http://dx.doi.org/10.1155/2015/292905

Research Article

Propagating Characteristics of Pulsed Laser in Rain

Jing Guo,[1] He Zhang,[2] and Xiang-jin Zhang[2]

[1]*School of IOT, Nanjing University of Posts and Telecommunications, Nanjing 210003, China*
[2]*ZNDY of Ministerial Key Laboratory, Nanjing University of Science and Technology, Nanjing 210094, China*

Correspondence should be addressed to Jing Guo; guojing@njupt.edu.cn

Received 28 March 2015; Revised 10 August 2015; Accepted 12 August 2015

Academic Editor: Ikmo Park

To understand the performance of laser ranging system under the rain weather condition, we need to know the propagating characteristics of laser pulse in rain. In this paper, the absorption and attenuation coefficients were calculated based on the scattering theories in discrete stochastic media, and the propagating characteristics of laser pulse in rain were simulated and analyzed using Monte-Carlo method. Some simulation results were verified by experiments, and the simulation results are well matched with the experimental data, with the maximal deviation not less than 7.5%. The results indicated that the propagating laser beam would be attenuated and distorted due to the scattering and absorption of raindrops, and the energy attenuation and pulse shape distortion strongly depended on the laser pulse widths.

1. Introduction

Laser detection becomes more and more important in remote measurement, for its highly monochromatic and coherent, high energy density and fine time resolution [1]. Meanwhile, it is also well known that light propagating in atmosphere is highly scattered by atmospheric hydrometeors and aerosols, occasionally causing an extreme high attenuation of the received power [2–6].

Rainfall is one of the most common types of precipitation. As pulsed laser propagates in rain, the interaction of light with raindrops, such as absorption and scattering, will take place, so the received signal is attenuated and distorted which leads to the degradation of laser ranging performance. Therefore, the investigation of light propagation in rain is an indispensable part of the design of the laser ranging system. Some pertinent propagation models are developed in the past researches. Wojtanowski et al. [7] analyzed the propagating characteristics of pulsed laser with wavelengths of 905 nm and 1550 nm in rain and fog. Lakshmi et al. [8] studied rain attenuation at 11 GHz based on the measured Drop Size Distribution (DSD). Choi [9] presented the measurement results of rain-induced attenuation at 12.25 GHz during some rain events; their measured results are in good agreement with the ITU-R prediction. Wang et al. [10] calculated the scattering phase functions for droplets and raindrops based on the Mie theory and compared the extinction measurements from Forward Scattering Visibility Meter (FVM) with those from manual observations during fog and rain. Dhawan and Singh [11] investigated the effect of the various atmospheric conditions including fog, snow, and rain on the FSO link. Some other studies combined the empirical relationships with the knowledge based on the theoretical analysis of light scattering in rain and fog [12–14]. While being sufficient for practical purposes, the available research results do not present the whole characteristics of the laser propagation in rain and these characteristics are very important to the design of laser ranging system. As a result, the propagating characteristics and energy attenuation of pulse laser in rain are comprehensively studied in this paper. The Monte-Carlo (MC) method is utilized to study the relationship of optical attenuation and the physical parameters of rain, and the controlled experiments are carried out to verify the theoretical simulation.

2. Propagation and Attenuation of Pulsed Laser in Rain

The performance of laser ranging system can be demonstrated by a laser ranging equation, which is commonly used to estimate the maximum detection range and influence

factors of ranging system. The optical echo power reflected by the target is provided by a classical ranging equation [15]:

$$P_R = \frac{P_T \tau_E \tau_R \tau_F A_R \rho \cos\beta}{\pi R^2} e^{-2\int_0^L \alpha(r)dr}, \quad (1)$$

where P_T is the peak power of emitting laser pulse, τ_E is the spectral transmission of emitting optics, τ_R is the spectral transmission of receiving optics, τ_F is the transmission of narrow band filter, ρ is the target's reflectivity coefficient, A_R is the receiving aperture area, β is the angle between the normal of target surface and the optical axis, R is the target distance, and $\alpha(\lambda, r)$ is the atmospheric extinction coefficient at distance r.

From (1), pulse echo characteristics are related to the process of laser propagation in atmosphere and reflection on the target surface. In order to track the target and measure its range in the complex atmospheric conditions (such as rain, dust storms, and fog), the influence of atmosphere must be considered.

2.1. Attenuation Coefficient of Laser in Stochastic Rainfall. When laser propagates in rain, the interaction of light with raindrops, such as absorption and scattering, will take place. The attenuation coefficient of laser in rain can be expressed as the following formula [16, 17]:

$$\alpha(\lambda) = \mu_s(\lambda) + \mu_a(\lambda), \quad (2)$$

where $\mu_s(\lambda) = \int_{D_1}^{D_2} \sigma_s(D)N(D)dD$ is the scattering coefficient and $\mu_a(\lambda) = \int_{D_1}^{D_2} \sigma_a(D)N(D)dD$ is the absorption coefficient. $N(D)$ is the function of raindrop size distribution, $\sigma_a(D)$ is the absorption cross section of raindrop, and $\sigma_s(D)$ is the scattering cross section of raindrop, which corresponds to the following equation [14]:

$$\sigma_s = \frac{\pi D^2}{4}\left[1 - {J_0}^2(\alpha) - {J_1}^2(\alpha) + \int_0^{\pi} \left(\varepsilon_1 \sin^2\varphi + \varepsilon_2 \cos^2\varphi\right) G \sin\theta \, d\theta\right], \quad (3)$$

where J_0 and J_1 indicate the Bessel functions of order zero and one, respectively, r_1 and r_2 are the Fresnel reflection coefficients, and θ is the scattering angle; τ and τ' refer to the coangles of incidence angle and refraction angle, respectively, φ is the polarization angle, and ε_j $(j = 1, 2)$ and G are given by

$$\varepsilon_j = \left(1 - {r_j}^2\right)^2$$
$$G = \frac{\sin\tau\cos\tau}{\sin\theta\,|d\theta/d\tau|} = \frac{\sin\tau\cos\tau}{\sin\theta}\left|\frac{1}{2 - 2tg\tau/tg\tau'}\right|. \quad (4)$$

Raindrop's absorption is relevant to the complex refractive index of water at a certain wavelength. The absorption cross section of raindrop can be expressed as multiplication of the absorbing efficiency factors $Q_{\text{abs}}(\lambda, D)$ and geometric cross section. The approximate calculation formula is as follows:

$$\sigma_a(\lambda, D) = \frac{\pi D^2}{4} Q_{\text{abs}}(\lambda, D) = \frac{\pi D^2}{4}\left\{\left[1 + \frac{\exp\left(-4xn_i(\lambda)\right)}{2xn_i(\lambda)}\right] + \frac{\exp\left(-4xn_i(\lambda)\right) - 1}{8x^2 {n_i}^2(\lambda)}\right\}. \quad (5)$$

According to (2)–(5), the scattering and attenuation coefficients of light with wavelength 1.064 μm at different rainfall rates are calculated and tabulated as shown in Table 1.

Table 1: Attenuation coefficients of different rainfall rate.

Rainfall	Rainfall rate (mm/h)	Scattering coefficient (m^{-1})	Attenuation coefficient (m^{-1})
Flurry	5.00	0.0013	0.00132
Moderate rain	12.5	0.0024	0.00244
Heavy rain	25.0	0.0038	0.00387
Rainstorm	100	0.0097	0.00991

2.2. Monte-Carlo Model for Pulsed Laser Propagating in Rain. When propagating in rain, collimated laser will be attenuated due to the absorption and scattering effects of the raindrops. Meanwhile, the path of laser beam may also be altered when the scattering event occurs, and after multiple scattering, the extended laser beam would be formed at the receiver. In addition, the trajectory length of beam in rain varies with different scattering paths, which is clearly greater than that of linear propagation direction, resulting in the propagating delay.

The laser beam can be regarded as a photon bundle that consists of massive photons, so the laser propagation can be treated as photon migration. In Monte-Carlo method, the interaction of photons with stochastic distributing particles is elastic scattering, and each photon will suffer multiple scattering [18–21]. The Monte-Carlo method is used to trace the propagation of large number of photons in rain; however these photons will be absorbed or scattered during this process. The trajectory of each photon is followed until it exits the medium or reaches the receiver. Then, the arriving time and position of the photons are recorded at the receiver to calculate the physical parameters that we need [22–24]. Figure 1 shows the schematic diagram for photons propagation model in stochastic rainfall.

The photon state is represented by three parameters, which are spatial location (x, y, z), migration direction (θ, φ), and weight w. Figure 2 shows the coordinates of photon propagation, of which, z-axis corresponding to the propagating direction, each photon migration is relevant to the previous interaction. Before proceeding to simulation, each photon will be initialized separately, and the initial weight w is set to $w = 1$.

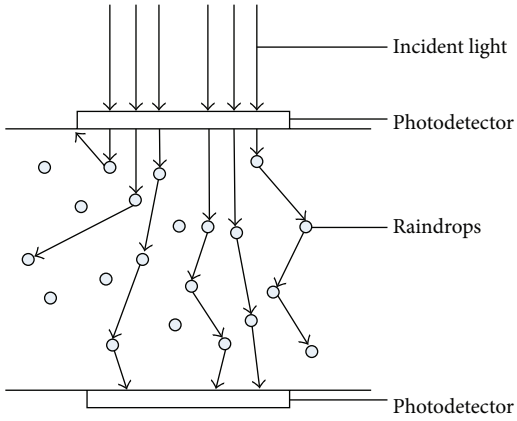

Figure 1: Schematic diagram for photons propagation model in stochastic rainfall.

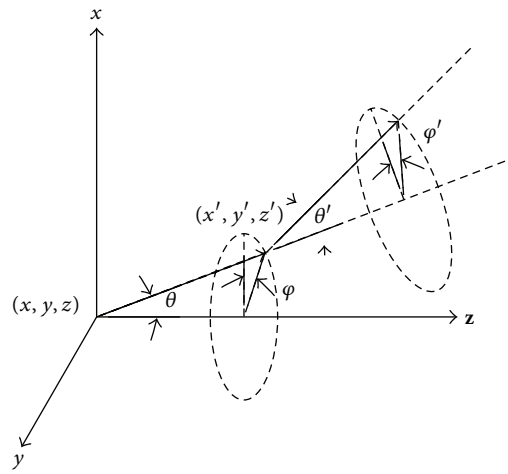

Figure 2: Coordinates of photon propagation.

A random migration of photons is executed between two interactions in Monte-Carlo simulation, and this free path length l is

$$l = \frac{-\ln \xi}{\mu_a + \mu_s}, \tag{6}$$

where ξ is a uniform random number in the interval $(0, 1)$. Once the free path length l is determined, the adjacent expected spatial location (x', y', z') can be obtained from the current spatial location (x, y, z) and the propagating direction vector (u_x, u_y, u_z); the formula is as follows:

$$\begin{aligned} x' &= x + u_x l \\ y' &= y + u_y l \\ z' &= z + u_z l. \end{aligned} \tag{7}$$

After a migration of the photon, its energy will be partly absorbed, leading to the decrease of its weight. The revised photon weight is expressed by

$$w' = w\left(1 - \frac{\mu_s}{\mu_s + \mu_a}\right). \tag{8}$$

When a photon is scattered and migrating to a new location, the new direction is randomly generated which is determined by azimuth φ' and scattering angle θ'. φ' is a uniform distributed angle in the interval $(0, 2\pi)$, and θ' can be obtained from Henyey-Greenstein phase function:

$$\theta' = \arccos\left\{\frac{1}{2g}\left[\left(1 + g^2\right) - \frac{\left(1 - g^2\right)^2}{\left(1 - g + 2g\xi\right)^2}\right]\right\}, \tag{9}$$

where g is anisotropy factor. After the photon collision, the new direction vector is updated by the following formulas:

$$\begin{aligned} u_x' &= \frac{\sin\theta'\left(u_x u_z \cos\varphi' - u_y \sin\varphi'\right)}{\sqrt{1 - u_z^2}} + u_x \cos\theta' \\ u_y' &= \frac{\sin\theta'\left(u_y u_z \cos\varphi' - u_x \sin\varphi'\right)}{\sqrt{1 - u_z^2}} + u_y \cos\theta' \\ u_z' &= -\sin\theta' \cos\varphi \sqrt{1 - u_z^2} + u_z \cos\theta' \\ &\qquad\qquad |u_z| < 0.99999. \end{aligned} \tag{10}$$

If the migrating direction is very close to z-axis, $|u_z| > 0.99999$, the new direction can be rewritten as

$$\begin{aligned} u_x' &= \sin\theta' \cos\varphi' \\ u_y' &= \sin\theta' \sin\varphi' \\ u_z' &= \mathrm{SIGN}\left(u_z\right) \cos\theta' \end{aligned} \tag{11}$$

$$\mathrm{SIGN}\left(u_z\right) = \begin{cases} 1 & u_z \geq 0 \\ -1 & u_z < 0. \end{cases}$$

3. Numerical Results from Monte-Carlo Simulations

By utilizing the above Monte-Carlo model, the propagating characteristics of pulsed laser in rain are numerically simulated. In the simulation, we assume that the laser signal is a Gaussian pulse and wavelength is $\lambda = 1064$ nm. The simulating photon number for pulse peak is set to $N = 10^4$. For the sake of clearly examining numerical results, the moment of pulsed peak of the initial signal and receiving signal was taken as the benchmark.

3.1. Influence of Rainfall Rate. To know the influence of different rainfall rates R on laser propagating characteristics, the pulsed laser propagating in rain with different rainfall

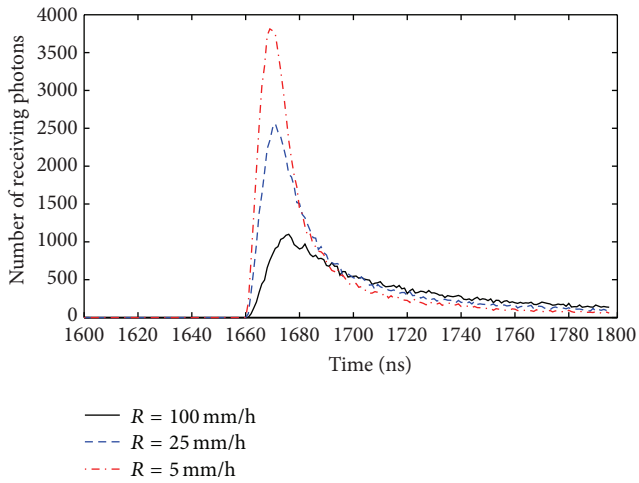

FIGURE 3: Temporal profiles of transmitted laser pulse for variable rainfall rates.

rates is simulated. Figure 3 shows the temporal profiles of transmitted laser pulse at variable rainfall rates. The initial pulse duration is 10 ns and the propagating distance is 500 m.

After the long-distance propagation, the initial pulsed signals are distorted due to the multiple scattering. The falling edge of waveform becomes gentle, like dragging a long "tail." It can be seen that the number of photons in the maxima decreases as R increases, the maximum number of photons in pulse shifts to larger times, the pulse width is broadened, and the "tail" becomes more pronounced. As R increases, the mean free path length l is shortened, resulting in the increase of the scattering events. Therefore, the trajectories deviate from the straight line more seriously , and then the propagation time and absorbed probability increase. Similar principles apply to the "tails."

3.2. Influence of Propagating Distance. Distance is also an important factor affecting the propagating characteristics of optical signal in rain. The temporal profiles of transmitted laser pulse for both propagating distances (50 m and 100 m) in rain ($\mu_s = 0.0038$/m and $\mu_a = 0.0007$/m) are shown in Figure 4. In the simulation, the initial pulse duration is 20 ns.

It is evident that the long distance can cause much larger attenuation and delay spread of optical signal on the atmospheric links. In Figure 4(a), the maximum number of photons of the scattered pulse is reduced to 8370. That means that the peak energy is attenuated by 16.3%. In addition, by comparing with the ideal signal, the pulse width is broadened to 21.5 ns and the peak time is delayed by 1 ns due to the effect of raindrop scattering. When the propagating distance increases to 100 m (Figure 4(b)), the maximum number of photons is reduced to 7601 and the energy attenuation is nearly 24%. Meanwhile, the pulse width is broadened to 22 ns and the peak time is delayed by 3 ns. From the simulation results, we can easily get the conclusion that, with the increase of propagating distance, the laser energy will be gradually attenuated and the pulse width and propagating delay increase. The phenomenon occurs due to the multiple

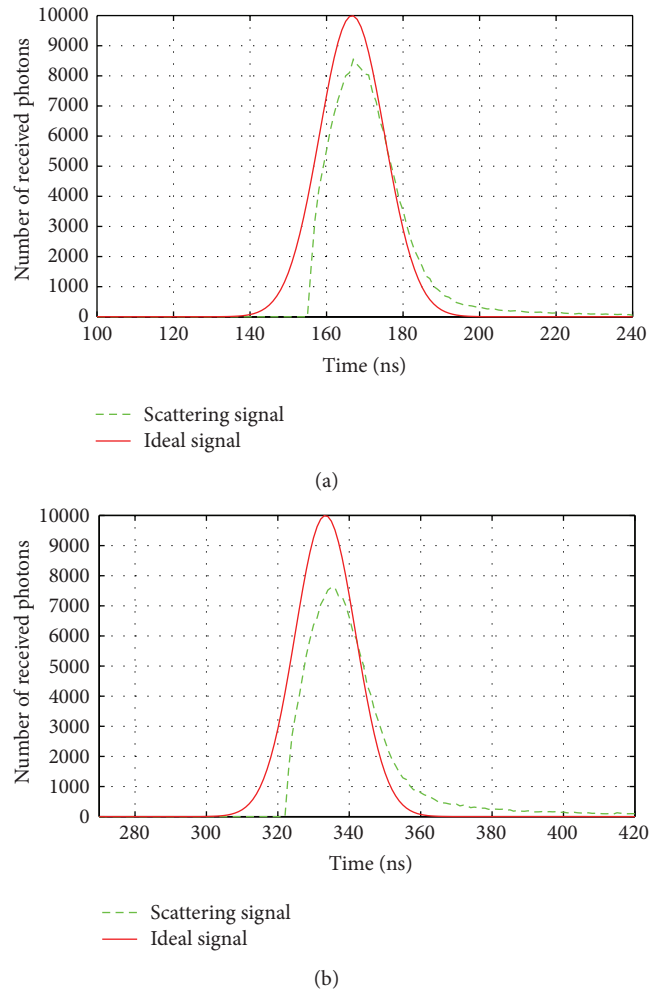

FIGURE 4: Temporal profiles of transmitted laser pulse for variable propagating distances ((a) 50 m; (b) 100 m).

scattering of photons, which makes their propagation path longer with respect to the distance between the transmitter and receiver. As a consequence, almost all the photons experience a large amount of scattering and absorption, which leads to the energy attenuation and delayed arriving of photons at the receiver.

3.3. Influence of Pulse Width. In order to compare the influences of different pulse widths on the propagating characteristics of pulsed laser, we make the assumption that the pulse energy of each pulse width is the same and the maximum numbers of photons of different pulse width can be obtained from formula $P = E/t$, where P is the pulsed peak power, E is pulse energy, and t is pulse width. If the maximum number of photons of 15 ns pulse is set to $N = 10^4$, the maximum numbers of photons which correspond to the pulse widths of 5 ns, 30 ns, and 50 ns are 3×10^4, 0.5×10^4, and 0.3×10^4, respectively. The temporal profiles of transmitted laser pulse of various pulse widths under the same 100 m propagating length in rain ($\mu_s = 0.0038$/m and $\mu_a = 0.00007$/m) are shown in Figure 5.

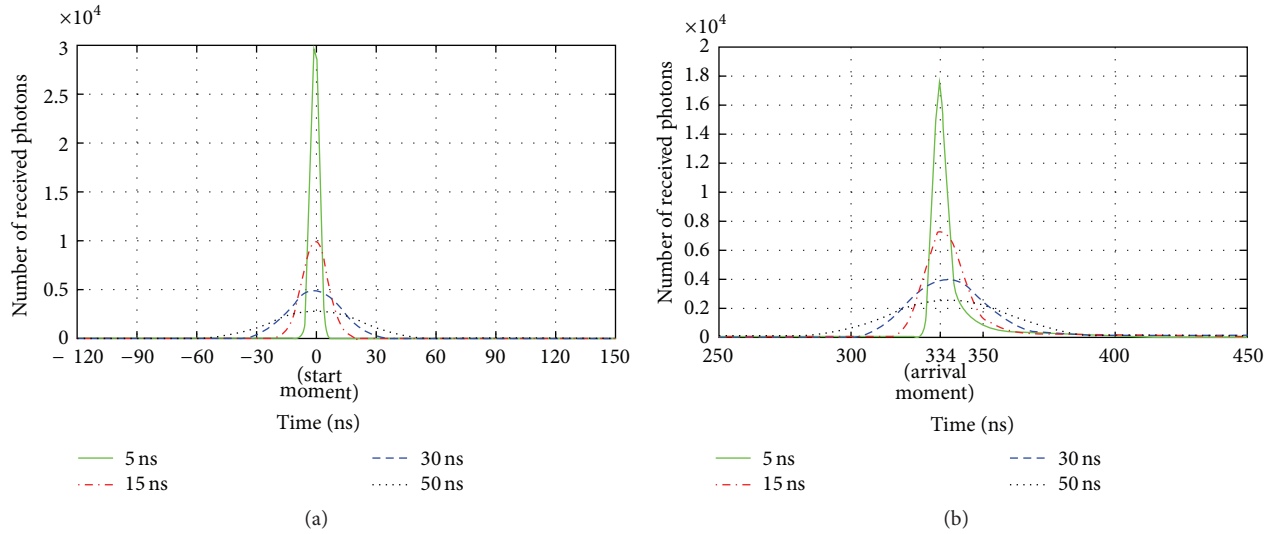

Figure 5: Temporal profiles of laser pulse of various pulse widths in rain ((a) initial signal; (b) received signal).

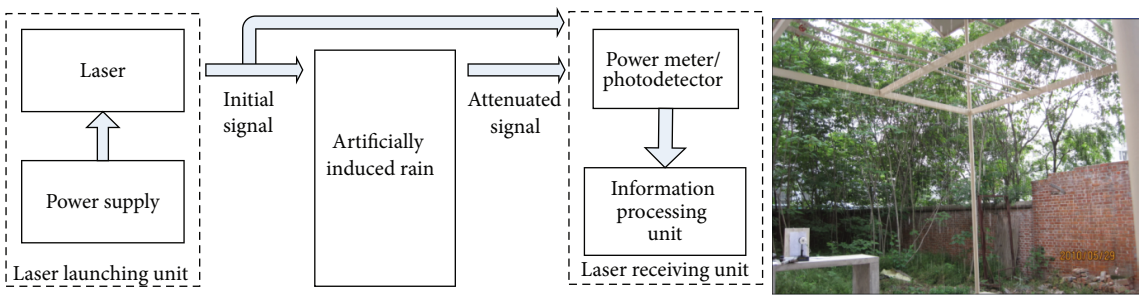

Figure 6: Experimental arrangement for determination of the rain's attenuation.

Table 2: Transmittance of peak energy for different pulse widths.

Propagating distance (m)	Pulse width (ns)			
	5	15	30	50
50	69.73%	82.23%	87.06%	91.03%
100	58.60%	73.84%	80.32%	86.63%

From Figure 5, short pulses have shorter delay than long pulses. For pulse durations of 5 ns, 15 ns, 30 ns, and 50 ns, the time delay is 2 ns, 3 ns, 4 ns, and 6 ns, respectively. The energy attenuation of short pulse is much greater than long pulse. The transmittance of peak energy of different pulse widths based on simulation data is tabulated in Table 2. It can be noted that the transmittances increase with the broadening of pulse width and decrease with the increase of propagating distance. For the signals with same pulse energy, the energy transmittance of short pulse is lower, but the peak energy is much higher than long pulse. From (1), we can infer that the greater the peak power, the better the detection performance. Therefore, short pulse is more superior for long-distance ranging system.

4. Experimental Results and Discussion

A control experiment is set up to verify the accuracy of simulation model. Figure 6 shows the experimental arrangement for determination of the rain's attenuation. This setup consists of laser generating pulses (λ = 1064 nm, average power P_{avg} = 15 mW, and repetition rate f = 10 KHz), a detection device equipped with high sensitive power meters (wavelength range: 0.19–2.1 μm, resolution: 10 μW, and active area diameter: 19 mm), and field artificial rainfall equipment (measurement error of rainfall: ≤2%, evenness of rainfall: >0.7, and resolution of rain gauge: 0.1 mm). The experimental devices can be placed on the fixed or mobile platform to fit different measuring distance. The artificial rainfall rate is adjusted to 25 mm/h and 100 mm/h, which corresponds to the scattering coefficients 0.0038/m and 0.0097/m from Table 1. The transmittance of laser pulse propagating in rain of various distances is measured; results are compared with the simulation for probability of received photons at the same condition. With emission pulse width of 20 ns, the simulation and experimental results of laser pulse propagating in rainfall of various distances are shown in Table 3. It can be seen that the maximum deviation between experimental data and simulation results is no more than 7.5%, which means that the

Table 3: Numerical and measured data of laser pulse propagating in rain for various distances.

Rainfall rate	Distance (m)					
	10		50		100	
	Calculation result	Experimental data	Calculation result	Experimental data	Calculation result	Experimental data
25 mm/h (0.0038)	91.7%	85.2%	83.7%	78.5%	76.1%	70.1%
100 mm/h (0.0097)	90.7%	83.4%	75.3%	70.2%	60.1%	54.5%

Table 4: Measurement value of signal peak power transmittance for different pulse width.

Propagating distance (m)	Pulse width (ns)			
	5	15	30	50
50	62.6%	80.3%	82.5%	85.6%
100	53.2%	69.8%	77.6%	80.7%

simulation model can precisely predict the process of light propagation in rain. It is also noticed that the experimental data is slightly less than the calculation result. The laser beam used in the experiment has a certain diameter, while the simulation model is approximately zero. The errors are generated by these differences.

The same control experiments are performed by adjusting the pulse width to 5 ns, 15 ns, 30 ns, and 50 ns, respectively, and the results are also compared with the simulation data. As shown in Table 4, the maximum deviation between measured data and simulation results (Table 2) is less than 7%.

5. Conclusions

The attenuation of light in rain has nonnegligible impact on the propagation characteristics of laser ranging systems applied in rain. The Monte-Carlo simulations of laser pulse propagating in rain and some experiments under specific rain were performed, and the deviation between the experimental data and simulation results is less than 7.5%. It has been concluded that attenuation and pulse delay increase with the rainfall rate and propagating distance. In addition, the pulse widths of propagating signals obviously affect the ranging performance. For the signals with same pulse energy, a short pulse has shorter delay but lower energy transmittance than a long pulse.

Conflict of Interests

The authors declare that there is no conflict of interests regarding the publication of this paper.

Acknowledgments

The research contained here was supported by National Science Foundation of China (Grant no. 60908037) and was financially supported by National Ministries of China (Grant no. 9140A05010610BQ02).

References

[1] K. V. Narasimham, M. Premasundaran, and C. L. Garg, "Laser technique applied to defence problems," *Defence Science Journal*, vol. 17, no. 4, 2014.

[2] M. Grabner and V. Kvicera, "Multiple scattering in rain and fog on free-space optical links," *Journal of Lightwave Technology*, vol. 32, no. 3, Article ID 6679219, pp. 513–520, 2014.

[3] Y. Ruike, H. Xiange, H. Yue, and S. Zhongyu, "Propagation characteristics of infrared pulse waves through windblown sand and dust atmosphere," *International Journal of Infrared and Millimeter Waves*, vol. 28, no. 2, pp. 181–189, 2007.

[4] S.-Q. Zhang, "The analysis of scattering effect for the transmission of 1.06 μm laser in lower altitude atmosphere," *International Journal of Infrared and Millimeter Waves*, vol. 28, no. 6, pp. 491–497, 2007.

[5] P. Singh and M. L. Singh, "Experimental determination and comparison of rain attenuation in free space optic link operating at 532 nm and 655 nm wavelength," *Optik*, vol. 125, no. 17, pp. 4599–4602, 2014.

[6] X. Sun, H. Wang, W. Liu, and J. Shen, "Nonspherical model for sand dust storm and its application to the research of light multiple scattering," *Acta Optica Sinica*, vol. 30, no. 5, pp. 1506–1510, 2010.

[7] J. Wojtanowski, M. Zygmunt, M. Kaszczuk, Z. Mierczyk, and M. Muzal, "Comparison of 905 nm and 1550 nm semiconductor laser rangefinders' performance deterioration due to adverse environmental conditions," *Opto-Electronics Review*, vol. 22, no. 3, pp. 183–190, 2014.

[8] S. Lakshmi, Y. H. Lee, and J. T. Ong, "The role of particular rain drop size on rain attenuation at 11 GHz," in *Proceedings of the 6th International Conference on Information, Communications and Signal Processing (ICICS '07)*, Singapore, December 2007.

[9] D. Y. Choi, "Measurement of rain attenuation of microwaves at 12.25 GHz in Korea," in *NETWORKING 2005. Networking Technologies, Services, and Protocols; Performance of Computer and Communication Networks; Mobile and Wireless Communications Systems*, vol. 3462 of *Lecture Notes in Computer Science*, pp. 223–233, Springer, Berlin, Germany, 2005.

[10] M. Wang, W.-Q. Liu, Y.-H. Lu et al., "Study on the measurement of the atmospheric extinction of fog and rain by forward-scattering near infrared spectroscopy," *Spectroscopy and Spectral Analysis*, vol. 28, no. 8, pp. 1776–1780, 2008.

[11] S. Dhawan and M. Singh, "To study the effect of fog, snow and rain attenuation on FSO link," *CT International Journal of Information & Communication Technology*, vol. 2, no. 1, pp. 16–22, 2014.

[12] S. Mori and F. S. Marzano, "Effects of multiple scattering due to atmospheric water particles on outdoor free space optical links," in *Proceedings of the 8th European Conference on Antennas and*

Propagation (EuCAP '14), pp. 1042–1045, IEEE, The Hague, The Netherlands, April 2014.

[13] V. Brazda, V. Schejbal, and O. Fiser, "Rain impact on FSO link attenuation based on theory and measurement," in *Proceedings of the 6th European Conference on Antennas and Propagation (EUCAP '12)*, pp. 1239–1243, IEEE, March 2012.

[14] A. K. Rahman, M. S. Anuar, S. A. Aljunid et al., "Study of rain attenuation consequence in free space optic transmission," in *Proceedings of the 6th National Conference on Telecommunication Technologies, and 2nd Malaysia Conference on Photonics (NCTT-MCP '08)*, pp. 64–70, IEEE, 2008.

[15] H. Zhang, J. Guo, and X.-J. Zhang, "Research of semiconductor pulsed laser spot shaping method," *Journal of Nanjing University of Science and Technology*, vol. 34, no. 5, pp. 592–601, 2010.

[16] Y.-J. Dai, *Principles of Laser Radar*, Defense Industry Publishing, Beijing, China, 2002.

[17] H. C. Van de Hulst, *Light Scattering by Small Particles*, Wiley, New York, NY, USA, 1957.

[18] J. Guo, H. Zhang, and X.-F. Wang, "Attenuation and transmission of laser radiation at 0.532μm and 1.064μm through rain," *Acta Optica Sinica*, vol. 31, no. 1, Article ID 0101004, 2011.

[19] J. Hu, Z. Yang, and D. Yang, "Smoke particles' recognition and Monte Carlo simulation of laser scattering character," *Chinese Journal of Lasers*, vol. 29, no. 10, pp. 950–954, 2002.

[20] A. P. Popov and A. V. Priezzhev, "Laser pulse propagation in turbid media: Monte Carlo simulation and comparison with experiment," in *Proceedings of the Saratov Fall Meeting 2002: Optical Technologies in Biophysics and Medicine IV*, International Society for Optics and Photonics, 2003.

[21] E. A. Bucher, "Computer simulation of light pulse propagation for communication through thick clouds," *Applied Optics*, vol. 12, no. 10, pp. 2391–2400, 1973.

[22] A. Sassaroli, C. Blumetti, F. Martelli et al., "Monte Carlo procedure for investigating light propagation and imaging of highly scattering media," *Applied Optics*, vol. 37, no. 31, pp. 7392–7400, 1998.

[23] Z. Guo, J. Aber, B. A. Garetz, and S. Kumar, "Monte Carlo simulation and experiments of pulsed radiative transfer," *Journal of Quantitative Spectroscopy & Radiative Transfer*, vol. 73, no. 2-5, pp. 159–168, 2002.

[24] R. Graaff, M. Koelink, F. de Mul, W. Zijlstra, and A. C. M. Dassel, "Condensed Monte Carlo simulations for the description of light transport," *Applied Optics*, vol. 32, no. 4, pp. 426–434, 1993.